



Published in final edited form as:

Brain Struct Funct. 2016 January ; 221(1): 487–506. doi:10.1007/s00429-014-0921-7.

Thalamic alterations in preterm neonates and its relation to ventral striatum disturbances revealed by a combined shape and pose analysis

Yi Lao, MS¹, Yalin Wang, PhD², Jie Shi, MS², Rafael Ceschin, MS³, Marvin D. Nelson, MD¹, Ashok Panigrahy, MD^{1,3}, and Natasha Leporé, PhD¹

¹Department of Radiology, University of Southern California and Children's Hospital, Los Angeles, CA 90027, USA

²School of Computing, Informatics, and Decision Systems Engineering, Arizona State University, Tempe, AZ 85281, USA

³Department of Radiology, Children's Hospital of Pittsburgh UPMC, Pittsburgh, PA, USA

Abstract

Finding the neuroanatomical correlates of prematurity is vital to understanding which structures are affected, and design efficient prevention and treatment strategy. Converging results reveal that thalamic abnormalities are important indicators of prematurity. However, little is known about the localization of the disturbance within the subnuclei of the thalamus, or on the association of altered thalamic development with other deep gray matter disturbances. Here, using brain structural magnetic resonance imaging (MRI), we perform a novel combined shape and pose analysis of the thalamus and ventral striatum between 17 preterm and 19 term-born neonates. We detect statistically significant surface deformations and pose changes on the thalamus and ventral striatum, successfully locating the alterations on specific regions such as the anterior and ventral-anterior thalamic nuclei, and for the first time, demonstrating the feasibility of using relative pose parameters as indicators for prematurity in neonates. We also perform a set of correlation analyses between the thalamus and the ventral striatum, based on the surface and pose results. Our methods show that regional abnormalities of the thalamus are associated with alterations of the ventral striatum, possibly due to disturbed development of shared pre-frontal connectivity. More specifically, the significantly correlated regions in these two structures point to frontal-subcortical pathways including the dorsolateral prefrontal-subcortical circuit, the lateral orbitofrontal-subcortical circuit, the motor circuit, and the oculomotor circuit. These findings reveal new insight into potential subcortical structural covariates for poor neurodevelopmental outcomes in the preterm population.

Keywords

Frontal-subcortical circuits; Pose; Prematurity; Subcortical structures; Tensor-based Morphometry

1 Introduction

Neonates born prematurely are at risk for cognitive, behavioral and social problems in later life (Wood et al., 2000; Marlow et al., 2005; Fily et al., 2006; Reijneveld et al., 2006; Hattie, 2008; Caravale et al., 2005). In the last decade, the role of frontal-subcortical circuits has been put forward in mediating executive functions, emotions and motivation, and have been investigated as a unifying framework in the studies of human neuropsychiatric disorders (Cummings, 1993; Mega and Cummings, 1994; Goldman-Rakic, 1987). In prematurity studies, the damage to cerebral white matter, especially in the frontal lobes, has been long recognized as a major cause of prematurity related poor neurological outcomes. Neurological disorders like attentional deficit/hyperactivity disorder (ADHD), autism spectrum disorders (ASD) and learning disabilities, which are common in preterm subjects, have been linked to disturbances of brain functions that can be ultimately attributed to the dorsolateral prefrontal circuit (DLPC), the lateral orbitofrontal circuit (LOFC) and the oculomotor circuit (Bechara et al., 2000; Sonuga-Barke, 2002; Toplak et al., 2005; Joseph and Tager-Flusberg, 2004; Robinson et al., 2009). The ventral striatum (putamen and globus pallidus) and the thalamus are paired deep gray matter structures involved in motor, cognitive, visual and sensory functioning, thus providing a potential seat for anatomical alterations underlying corresponding neurological dysfunctions. The vulnerability of these two structures to prematurity or prematurity associated complications has been investigated in previous works, with reduced volume reported in both structures (Nagasunder et al., 2011; Boardman et al., 2006, 2010; Inder et al., 2005; Peterson et al., 2000; Kesler et al., 2004, 2008; Abernethy et al., 2004; Shi et al., 2013). However, the investigation of neuroanatomical and functional correlations in the presence of prematurity has been confined almost entirely to the cerebral cortex, while the role of subcortical structures within specific frontal-subcortical circuits is poorly understood. In addition, studies to date have not looked at the structural covariance between subcortical structures like the thalamus and the putamen in preterm neonates.

As proposed by the concept of ‘encephopathy of prematurity’, the process of fetal brain development is accomplished by a series of complex and linked events, and disturbances or injuries in one part of the brain may lead to impaired functioning of other interconnected regions (Volpe, 2009; Hart et al., 2008). Animal studies (Groenewegen and Berendse, 1994; Haber, 2003) and diffusion tensor tractography techniques (Klein et al., 2010) provide descriptions of the topographical connections between subcortical areas and the cortex, and have showed that neuroanatomical subparcellations of deep gray matter structures can be linked to dedicated functional regions on the cortex. Given the functional and anatomical connections between the ventral striatum, the thalamus and the frontal lobes, a ‘trans-synaptical’ disturbance on the development of one or more in-circuit compartments may form a neuroanatomical substrate for circuit related neurological dysfunctions. Thus, a circuit wise investigation should not only capture more fully the spectrum of deep gray matter alterations due to prematurity, but also reveal the particular relevance of deep gray matter abnormalities to potential neurological outcomes. As the ventral striatum and the thalamus are two of the subcortical structures most commonly affected by prematurity, analyzing their related vulnerability to prematurity within the framework of frontal-

subcortical circuits is crucial to our understanding of impaired brain development, and for guiding circuit-specific early interventions.

Frontal-subcortical circuits mediate different functions via segregated but integrated pathways, with neuron fibers interdigitating specific nuclei of the thalamus and ventral striatum, rather than overlapping them (Cummings, 1993). As a result, to gain more insights on the altered development of frontal-subcortical circuits in preterm infants, anatomical abnormalities need to be localized at the level of subdivisions of the thalamus and ventral striatum. However, the traditional volumetry method does not provide regional specificity on the subcortical structures, while whole brain deformation-based morphometry (Boardman et al., 2006; Ball et al., 2012) findings consist in abnormalities that are not well localized within subcortical structures and, additionally, are prone to registration artifacts – a non-negligible effect in gray matter near the ventricles. This highlights the need for more sensitive methodologies, and for a detailed assessment of the subtle morphometric structural changes caused by prematurity.

In our previous work, we extended the traditional univariate surface based morphometry (Wang et al., 2010a) to a multivariate version that has shown greater statistical power to detect population differences in subcortical structures, both in neonates (Wang et al., 2011b; Shi et al., 2013) and in adults (e.g. Wang et al. (2011c); Wang et al. (2010a)). Complementary to the surface based shape analysis, the relative pose of subcortical structures may also help to indicate abnormal growth of the brain (Lao et al., 2013). The relative pose is the residual position of the subcortical structure (translation, rotation and scale relative to an average shape) after removing irrelevant external information such as the arbitrary location of patients' head within the scanners and the size of the head. This information is especially important in depicting the development or degeneration patterns of the brain, when shifts of pose in different subcortical structures are more likely to happen, secondary to the volume and shape changes of neighboring structures. The relative pose is complementary to subcortical surface shape analyses, and the combined shape and pose results form a complete subcortical morphometry system. However, few attempts have been made to perform surface based statistics on subcortical structures in preterm neonates (Shi et al., 2013). Moreover, there are few relative pose analyses in the field of neuroimaging (Bossa and Olmos, 2006; Gorczowski et al., 2010; Bossa et al., 2011), and to the best of our knowledge, none have focussed on neonates.

Despite their joint involvement in fronto-subcortical circuits, the linked involvement of the thalamus and ventral striatum in preterm associated injury remains understudied. In the handful studies that integrate both deep gray matter structures, Lin et al. (2001) reported reduced volume in both lentiform and thalamic nuclei in preterm neonates with periventricular leukomalacia (PVL). Srinivasan et al. (2007) confirmed the reduced lentiform and thalamic volume in preterm subjects with nonfocal white matter abnormalities. However, these studies are not powerful enough to reveal regional disturbances on the gray matter structures, and none of them have attempted to examine the associated disturbance between different deep gray matter structures. In our recent study investigating surface deformations of the ventral striatum (Shi et al., 2013), we found altered anterior and inferior part of the putamen in preterm newborns, but whether this involvement

of the ventral striatum in prematurity is due to a secondary effect of injury to the thalamo-cortical projections, or to impaired primary putaminal functions remains unknown. Thus, analyzing the associated alterations within these two gray matter structures may allow a refinement of the neurological model for the impaired developmental mechanisms of prematurity.

Here, we focus on examining the effect of prematurity on the thalamus and on investigating the linked disturbances in the ventral striatum. Our aim is two-fold: First, using brain structural magnetic resonance imaging (MRI), we apply a novel pipeline that integrates multivariate surface based morphometry and relative pose analyses, to fully capture the subtle alteration of deep gray matter development in preterm neonates. Here we focus more specifically on neonates with no visible evidence of white matter injury, to assess the power of our method to detect subtle abnormalities. Fig. 1 illustrates our surface generation and pose analysis pipelines. Secondly, we investigate the thalamic changes in relation to those of the ventral striatum using the information resulting from the combined shape and pose analysis. Our method extends knowledge gained from traditional volume based analyses of neonates in the literature, and provides anatomical evidence to the concept of ‘encephalopathy of prematurity’ as proposed by (Volpe, 2009). Our results indicate that surface morphology as well as pose information in subcortical structures may be sensitive indicators of brain injury and/or abnormal brain development.

2 Subjects and Methods

Fig. 1 illustrates our pipelines of point distribution model (PDM) generation, surface based morphometry and relative pose analysis.

2.1 Subjects and preprocessing

2.1.1 Neonatal Data—Our dataset comprises 17 premature neonates (gestational ages 25–36 weeks, 41.12 ± 5.08 weeks at scan time) prospectively recruited with normal MR scans and 19 healthy term born infants (gestational ages 37–40 weeks, 45.51 ± 5.40 weeks at scan time). T1-weighted MRI scans were acquired using a dedicated neonatal head coil on a 1.5T GE scanner using a coronal three-dimensional (3D) spoiled gradient echo (SPGR) sequence. The inclusion criteria for our preterm subjects were the following: 1) prematurity (less than 37 gestational weeks at birth), and 2) visually normal scans on conventional MR imaging. All subjects with visible injuries were excluded from the dataset. Structural MRI images were qualitatively classified as normal by 2 board certified neonatal neuroradiologists. Preterm subjects were excluded based on abnormal neurological exam, or if they exhibited brain lesions including: (1) focal or diffuse white matter injury (2) ventriculomegaly and (3) significantly increased subarachnoid space and sulcal enlargement. The institutional review board at our medical center approved the study protocol.

2.1.2 3D surface representations and registration—All the T1-weighted MRI scans were first registered to a template space through linear registration. Alignment quality was validated by superimposing images from different subjects on top of each other. Irrelevant global pose difference induced by different locations and orientations during scans was factored out in this step. The thalami and putamen were then manually traced on linear

registered T1 images by an experienced pediatric neuroradiologist using Insight Toolkit's SNAP program (Zhang et al., 2006). The intra-rater percentage overlap were 0.93 and 0.86 for measuring the thalamus and the putamen, respectively, in four participants at two subsequent times (two preterm and two term born participants).

3D surface representations of the segmented structures were constructed with marching cube algorithm. We included the putamen and globus pallidus in our ventral striatal surface reconstruction, due to the lack of tissue contrast on neonatal T1 images between these two structures. Given the large variability of brain morphology in neonates, the registration should allow for large deformations. Here, we non-linearly registered all subjects using a new surface fluid registration algorithm (Shi et al., 2012), which outperforms the more commonly used constrained harmonic registration, as compared in our previous work (Shi et al., 2013). The one-to-one correspondence achieved between vertices allows us to accurately analyze localized information on the surfaces of subcortical structures.

2.2 Surface based morphometry analysis

We perform a vertex-wise multivariate statistical analysis, including:

1. The distance ρ from a medial axis to a vertex on the surface (MAD) – which represents the thickness of the shape at each vertex (Pizer et al., 1999; Thompson et al., 2004). More precisely, the medial axis is computed using the center point on the iso-parametric curves, i.e. the iso-parametric curve is perpendicular to the medial axis, on the computed conformal grid (Wang et al., 2011c), after which ρ is easily found at each vertex.
2. The logged deformation tensor ($\log \sqrt{JJ^T}$, where J is the Jacobian matrix) (Wang et al., 2011a), as in our prior multivariate tensor-based morphometry (mTBM) analyses (Lepore et al., 2008; Wang et al., 2010a, 2011a), – which describes the directional differences in regional surface area between each subject and the template.

MTBM is complementary to MAD, as the radial distance primarily measures changes in thickness while the deformation tensors mainly capture changes in surface area, so we combine them in one multivariate 4×1 vector for analysis. Simpler univariate statistical analyses of ρ and of the determinant of the Jacobian matrix ($\det J$, the difference in surface area without directional information), as well as multivariate statistics on the deformation tensors alone are also conducted for comparison and validation.

Although the mean and distribution of age was roughly matched between preterm and term groups, subjects were scanned over an age range of 36–57 post-conception weeks. This variation of age is not negligible, especially for neonates whose brains change rapidly with age. The growth of the thalamus in neonates in terms of the volumetry and outgoing trajectory is approximately linear (Ball et al., 2012), thus we used linear regression to factor out the influence of age. Subsequent statistical analyses are performed on age-covaried data.

T -tests are used for the univariate measures. For either of the multivariate tests (mTBM or MAD + mTBM), multivariate statistics are computed using the Hotelling's T^2 test

(Hotelling, 1931) – the multivariate extension of the Student's t -test, as described in (Lepore et al., 2008; Wang et al., 2010a, 2011c).

We run two permutation tests on the images: a vertex-based one that allows us not to assume a normal distribution, and one over the whole segmented image to correct for multiple comparisons (Nichols and Holmes, 2001; Lepore et al., 2008; Wang et al., 2010a). The procedure is repeated 10,000 times. For the first permutation test, we obtain a null distribution of T^2 -values at each vertex to which we compare the T^2 -values from the real data. For the second one, we compute a single value over the whole image for each of the 10,000 permutations. The value we choose is $N_p^i = \text{number of } p\text{-values} < 0.05 \text{ over all vertices in the image for permutation } i$. This provides us with a null distribution to which we compare N_p^{true} from the true labels.

2.3 Relative pose analysis

We compute the relative pose for each of the four structures (left thalamus (LTha), right thalamus (RTha), left putamen (LPut), and right putamen (RPut)). This is done by full Procrustes alignment of each subject's surface to a template shape – that is by rotating, translating and uniformly scaling the subject's shape to align it with the template (Dryden and Mardia, 1998). The template is selected as the mean shape that minimizes Procrustes distances, and is computed iteratively (Ross, 2004). All transformations are centered on the center of mass of the template. To simplify the computation of statistics, these transformations are then projected onto the tangent plane at the origin of the manifold of transformations, in which simple flat space calculations can be performed (Arsigny et al., 2006). This is done using matrix logarithms, as in (Bossa and Olmos, 2006).

The mean pose m for the preterm and control groups can be calculated iteratively as (Karcher, 1977; Bossa et al., 2011; Pennec et al., 2006) After the subtraction of the mean from each subject's individual pose each subject is left with a residual pose. Statistics are computed on this residual pose which consists of 7 parameters: 1 scale, 3 rotations and 3 translations.

As was done in the surface based morphometry feature vectors, we used linear regression to factor out the influence of age on pose parameter. The distributions of pose parameters for 4 subcortical structures are shown in Fig. 2. To save space, only the data of the parameter $\log S$ are presented. Subsequent statistical analyses were performed on age-covaried data. Statistical comparisons between the two groups are performed via two methods: univariate t -tests for $\log S$, $\|\log R\|$, $\|\log d\|$; Multivariate Hotelling's T^2 -test, which is a multivariate generalization of the t -test, for 3 rotation parameters (θ_x , θ_y , θ_z), 3 translation parameters (x , y , z), as well as a combination of all 7 parameters.

For multiple comparisons, we randomly permute the labels of our subjects (preterm vs. term neonates), and generate t -values (for t -test) or F -values (for T^2 -test) for comparison. We use 10,000 permutations for each of the parameters to assemble a null distribution of non-parametric estimation for t - or F -values.

2.4 Correlation analysis

To test the hypothesis that thalamic abnormality is associated with that of the putamen, two kinds of correlation tests are performed on our previously obtained surface based information and pose parameters.

2.4.1 Surface morphometry correlation—To investigate regional correlation of the thalamus and the putamen, a correlation analysis is performed between the determinant (surface area) or medial axis distance (thickness) of each vertex on the thalamus with the total volume of the two putamen. A similar test is performed on the putamen, covaried with the total volume of the two thalami.

2.4.2 Relative pose statistics correlation—In order to further explore the association between the thalamus and the putamen, in terms of the trend of changes in position, we run a series correlation tests on the pose parameters between the four structures: LPut vs. LTha, RPut vs. LTha, LPut vs. RTha, RPut vs. RTha. The pose parameters that we test include: $\log S$, $\|\log R\|$, $\|\log d\|$, representing the scale, total rotation, and total translation of each structure.

3 Results

3.1 Surface morphometry analysis results

Fig. 3 displays areas of significant abnormality on the thalamus when comparing the preterm vs. term groups. Broad areas of significance are seen in the anterior and ventro-anterior parts of the two thalami, while the main cluster resides in the anterior-dorsal part of the left thalamus. All four methods agree as to the location of clusters of significance, though the mTBM results are a bit noisier than those for MAD or the determinant of Jacobian (detJ). However, the overall p -value for MAD and detJ are above the threshold for statistical significance – which we set here at $pt=0.05$, given our a priori hypothesis on the thalamus, while that for mTBM is much lower than pt . Both the FDR and permutation tests show that the combined analysis is the most powerful one. This is in line with our previous work with the putamen (Shi et al., 2013), in which significant regional differences are detected more extensively using multivariate measures.

In order to see the direction of the changes, we also map

$$R_{\text{det.J}}^k = \frac{\frac{1}{N_p} \sum_i^{N_p} \det J_{p_i}^k}{\frac{1}{N_c} \sum_j^{N_c} \det J_{c_j}^k} \quad (3)$$

and

$$R_{\rho}^k = \frac{\frac{1}{N_p} \sum_i^{N_p} \rho_{p_i}^k}{\frac{1}{N_c} \sum_j^{N_c} \rho_{c_j}^k} \quad (4)$$

at each voxel k (see Fig. 4), where $J_{p_i}^k$, $J_{c_j}^k$, $\rho_{p_i}^k$, $\rho_{c_j}^k$ are the Jacobian matrices and radial distances for the preterm or term-born subject i , respectively. N_p and N_c are the numbers of

preterm and term-born subjects. The determinant of the Jacobian matrix indicates the difference in surface area of the region in the individual subject compared to the template, while the radius measures change along the surface normal direction (thickness). In both ratio maps, values smaller than 1 indicate trophic changes at a given vertex in preterm group, and vice-versa for values greater than 1. As expected, the majority of the surface area shows an atrophic tendency in the preterm group. The anterior side of both thalami is smaller in the preterm group, although the area does not reach significance on the right thalamus. Furthermore, the pulvinar is smaller on average in our preterm subjects compared to the controls, a region that has previously been implicated in prematurity related thalamic injury (see e.g. Nagasunder et al. (2011)).

To get a more complete view of the ventral striatum, we also show the determinant and radius map for the putamen. In Fig. 5, we can also see a widespread atrophy in both of the putamen, with a more uniform distribution as compared to that of the thalamus. These results are consistent with neuroanatomy findings that the thalamus is more anatomically sub-dividable than other gray matter structures (Volpe, 2009).

3.2 Relative pose analysis results

All the p -values from previously described tests are presented in Table 1. For the left thalamus, pose parameters representing scale and rotation show a significant difference between the preterm and term groups, while no difference can be seen in translation parameters. It is also important to note that, apart from the difference detected in individual parameters, a combination of all 7 parameters also detects significant differences between the two groups in the left thalamus, indicating a possibility of using multivariate analysis of all pose parameters as the discriminant between the two populations. For the right thalamus, neither the individual nor combination of parameters detects any changes. For the left putamen, low p -values are seen in univariate scale and translation, as well as multivariate rotation parameters, but none of them reaches significance. For the right putamen, significant group difference are only seen in the scale parameter.

These results are better visualized in Fig. 6, where mean shapes of preterm (represented in red) vs. term (represented in blue) groups are overlaid in their corresponding mean pose. Areas where the mean shapes of two groups are overlaid appear in purple. Note the borders of these two structures: a shift in pose is evident on the left thalamus and putamen, while less visible variants appear on in right hemispheric structures. The left thalamus of the preterm group shows a smaller size, with the posterior part positioned more medially compared to the control group, which are consistent with the differences found in scale and rotation parameters. Compared to the obvious differences in size and shape, the shift of position of the left thalamus in these two groups are less evident, consistent with the results from our statistical tests. As for the left putamen, we can see a laterally shift in position along with a moderate difference in size, as is confirmed by the low p -values in all three sets of pose parameters. In the right hemisphere, the pose differences in both structures are less evident: mean shapes for the right thalamus from the two groups are mostly overlapped, in agreement with the relatively high p -value found in all pose parameters, while only a

shrinkage in size is evident in the right putamen, which is validated by the significance in its scale parameter.

3.3 Correlation results

3.3.1 Surface morphometry correlation—In Fig. 7 and Fig. 8, several subdivisions of the thalamus are significantly correlated with the volume of the putamen, such as the ventral anterior nucleus, medial dorsal nucleus and pulvinar. The same regions have been reported to be interconnected with the putamen and pallidum (also included in our putamen model) by a probabilistic tractography study (Draganski et al., 2008). However, these regions have different levels of shrinkage as shown in the group average determinant and radius maps, but only the ventral anterior nucleus reach a significance in the group difference map, as shown in Fig. 3.

As for the putamen, broad anterior and inferior areas, especially the anterior putamen and pallidum, are significantly associated with the volume of the thalamus. These are also in line with the previously mentioned theoretical study (Draganski et al., 2008), in which anterior putamen and pallidum, along with certain nuclei of the thalamus, are demonstrated to be concomitantly involved in several cortical-striatal-thalamo-cortical loops. Furthermore, these regions are largely overlapped with the significant group differenced areas, as previously found by our group (Shi et al., 2013). This suggests that the vulnerability of the putamen to prematurity is possibly a secondary effect of the thalamic injury.

3.3.2 Relative pose statistics correlation—As shown in Fig. 9, there are significant correlations ($p < 0.01$) between the left thalamus and the left putamen in terms of $\log S$ and $||\log d||$. A similar association exists in the right hemisphere, but to a lesser extent. Detailed correlation coefficients and their corresponding p values are presented in Table 2. All p -values are corrected using 10,000 permutations (see Sect. 2.3.2). Significant p -values ($p < 0.01$) are highlighted in pink.

4 Discussion

We applied a novel shape and pose combined analysis on the paired deep gray matter, the putamen (including the globus pallidus) and the thalamus, to compare the surface and relative pose changes between premature neonates and term born controls. Using surface based morphometry analysis, we detected widespread putaminal areas of significance group differences (Shi et al., 2013), as well as focal and regional involvement of anterior and ventral thalamic regions. All measures gave consistent results, and as expected, the combined (MAD-mTBM) statistic showed the highest detection power. Using relative pose analysis, we also detected significant positional differences in the left thalamus and the right putamen, as well as trends in the left putamen. In addition, our data showed a significant structural covariance between thalamus and putamen, with regional involvement of the ventral anterior, ventral posterior, dorsal medial and posterior of the thalamus, as well as anterior and inferior areas of the putamen. The same regions have been demonstrated to have neuronal fibers interconnecting these two structures (Draganski et al., 2008). Moreover, we tested the correlation of the pose parameters between the thalamus and the putamen, and found a strong association of the pose changes between these two structures.

Our findings further validate an intimate correlation of these two structures in the presence of prematurity, possibly underlying the disturbances of preterm delivery on the cortico-striato-pallido-thalamo-cortical circuits that involve both the ventral striatum and the thalamus.

4.1 Sensitivity of our methodology

Finding neuroanatomical indicators for abnormal development is necessary for timely therapeutic intervention, but is poorly achieved by current clinical measurements. Prior to this study, thalamic and putaminal volume reductions in preterm infants were reported by several volumetry and DBM studies (Nagasunder et al., 2011; Boardman et al., 2006, 2010; Inder et al., 2005; Kesler et al., 2004, 2008; Abernethy et al., 2004). While the majority of above prematurity studies focus on populations with PVL, poor neurodevelopmental outcomes are persistently presented in premature populations without focal brain injuries at birth (Grunau et al., 2002; Caravale et al., 2005; Hattie, 2008). In the few studies that zoom in on brain anatomic alterations in preterm populations without visible white matter injuries, Allin et al. (2004) performed voxel based analysis on a cohort of adults with very low birth weight and found a significant correlation between increased lateral ventricle and decreased gray matter, including caudate and thalamus, while no significant between-group difference in the whole brain grey matter was detected. Srinivasan et al. (2007) reported reduced volume of the thalamus and lentiform nucleus in preterm infants, and the reduction persists, but to a lesser extent, when participants with supratentorial lesions were excluded. These findings indicate that neuroanatomical alterations caused by the prematurity itself, while less extensive than associated perinatal brain injuries, are greater than previously assumed.

In this work, we exclude subjects with visible gray or white matter injuries and focus on analyzing the effects of prematurity itself. The vulnerability of the thalamus is confirmed by both the surface based statistic and relative pose analysis, and to be more specific, with the main surface differences seen in the anterior, ventral anterior (VA) nucleus of the thalamus (Fig. 3) and pose shift co-localized on the anterior/posterior poles (Fig. 6). In addition, significantly abnormalities of the anterior and inferior surface of the putamen are described in our previous publication (Shi et al., 2013), while significant pose differences on both putamen are first reported here. These findings provided new anatomical evidence for the importance of early detection of prematurity associated brain abnormalities and early clinical intervention. The relevance of detected abnormalities in this study to their underlying functional parcellation will be described in details in the next section.

4.2 Selective vulnerability of preterm birth

4.2.1 Cortico-striatal-pallido-thalamo-cortical circuits—Although the joint contribution of the thalamus and the putamen to altered brain development has not been described in previous prematurity studies, certain of their association features were proposed in (Volpe, 2009) and connectivity based studies in health adults (Draganski et al., 2008). Here, the close relationship between the thalamus and putamen related to preterm birth is validated by the correlation on pose parameters (Table 2), where scale and translation of the left putamen are significantly correlated with that of the left thalamus, and right thalamus and putamen are significantly associated through rotation. Additionally, as shown in our

surface based correlation analysis, several regions on the surface of the thalamus are significantly correlated with reduced putaminal volume, such as the ventral anterior (VA), inferior medial to posterior area (potentially embedded centrum medianum (CM) and parafascicularis (Pf)), as well as pulvinar. For the putamen, clusters that are significantly correlated with thalamic volume are primarily located in the anterior and inferior regions of the putamen surface. The regions mentioned above have all been previously demonstrated to have interconnections between the thalamus and putamen (Draganski et al., 2008; Metzger et al., 2013), and can be co-localized to several major frontal-subcortical circuits, including: the dorsolateral prefrontal-subcortical circuit (DLPC), the lateral orbitofrontal-subcortical circuit (LOFC), the motor circuit, and the oculomotor circuit. All of the above have the participation of both the ventral striatum and the thalamus.

The DLPC and LOFC originate from the prefrontal cortex, outflow via the basal ganglia, thalamus, and project back to the circuits' origins. These closed loop connections can be further divided into 'direct' and 'indirect' pathways. The direct pathway relays inhibitory GABA fibers from the caudate nucleus, and output via the globus pallidus interna (Gpi) to the ventral anterior (VA) thalamus, while the indirect pathway alternatively unites the globus pallidus externa (Gpe), the subthalamic nucleus (STN), and the Gpi, before the projections return to the medial-dorsal (MD) thalamus (Cummings, 1993; Mega and Cummings, 1994). From our correlation results (shown in Fig. 7, Fig. 8), both Gpi and Gpe of the putamen are significantly associated with thalamic volume, and at the same time, VA of the thalamus presents significant correlations with putaminal volume. These are indirectly validating the existence of the DLPC and LOFC. Moreover, significant group differences between our preterm and term neonates are seen in the VA of the thalamus, as well as in the Gpi and Gpe of the putamen, indicating that the DLPC and LOFC are at risk in preterm birth.

The DLPC has been identified as promoting executive function by substantial animal and fMRI studies, while the LOFC is thought to be associated with social restraint and empathy (Alexander et al., 1991; Cummings, 1993; Mega and Cummings, 1994). Emerging studies have shown that prematurity is a risk factor leading to attentional deficit hyperactivity disorder (ADHD) (Reijneveld et al., 2006; Bhutta et al., 2002), autism spectrum disorders (ASD) (Limperopoulos et al., 2008; Buchmayer et al., 2009), and global cognitive abnormalities (Caravale et al., 2005; Hart et al., 2008). These symptoms are usually considered as frontal lobe syndromes, and have been ultimately attributed to DLPC and LOFC dysfunctions. More specifically, ADHD is viewed as a disorder of cognitive and motivational regulation, and arises from an imbalance of the dual pathways system involving ventromedial prefrontal cortex and orbital frontal cortex (Bechara et al., 2000; Sonuga-Barke, 2002; Toplak et al., 2005). ASD was demonstrated to link with impaired executive function (Joseph and Tager-Flusberg, 2004; Robinson et al., 2009), reduced anterior thalamic radiation (Cheon et al., 2011) and frontal cortical dysplasias (Casanova et al., 2013). The significantly shrunk and highly correlated Gpi, Gpe of the ventral striatum and VA of the thalamus, as detected by our study, provide additional anatomical support to the involvement of the DLPC, LOFC in preterm birth. Our results further suggest that the altered development of these frontal-subcortical circuits may form the neuroanatomical basis for poor cognitive and socialization outcomes often seen in adolescent born preterm.

The motor and oculomotor circuits are two major frontal-subcortical circuits subserving motor functions, and united to the same subcortical members as DLPC/LOFC. In these two circuits, projections from the frontal cortex are topographically connected with the dorsal lateral putamen, Gpi, Gpe, VA and MD of the thalamus. As detected by our study, all the subcortical subparcellations mentioned above, except for the MD part of the thalamus, showed significant putaminal-thalamic correlations as well as significant group differences, making motor circuit and oculomotor circuit two putative locations for prematurity associated disturbances. The vulnerability of motor circuit and oculomotor circuit are also implied by clinical and research observations: faulty motor excitability and visuomotor coordination were observed in subject born very preterm (Flamand et al., 2012); delayed smooth pursuit movements were detected in preterm infants at 2 and 4 months corrected age (Strand-Brodd et al., 2011). These are all hallmarks of motor and oculomotor circuits disturbances. Our results add to this part of literature by providing *in vivo* anatomical support to the involvement of motor and oculomotor circuits in preterm birth. Nevertheless, more direct connectivity research is needed in the future to substantiate our findings.

In addition, it is important to note that MD of the thalamus, a major nucleus that has been previously demonstrated to be involved in all the frontal-subcortical circuits (Cummings, 1993; Mega and Cummings, 1994), did not present much correlation with the ventral striatum volume from our results. This is not unexpected, as the MD is the major relay hub of the thalamus and is embedded in numerous cortical-subcortical circuits, and therefore, reciprocally connected to additional subcortical members and the cortex. The co-existence and interaction of different neuro-circuits make it difficult to segregate one from another (Casanova et al., 2013; Golden and Harding, 2010). When considering the net effect of the potential hypoconnectivity from one circuit and wrongly wired neurons migrated from another, an increase in the latter would tend to balance a reduction in the former, thus hindering the detection of the correlation between MD thalamus and any specific members in the circuits, including putamen. Further supplementary studies, for instance a direct tractography study seeding on the putamen and MD of the thalamus would be a validation on the hypotheses derived here.

4.2.2 Other circuits harboring the thalamus—In Fig. 3, the preterm group presents a significant atrophy within the anterior part (AM, AD and VA) of the left thalamus, while only the VA is shown to be associated with putaminal disturbances, as described above. This suggests an influence of prematurity on some additional neuro-circuits encompassing the anterior nuclei of the thalamus, but without the participation of the ventral striatum. Unlike other association thalamic nuclei (i.e. MD and pulvinar) that were extensively investigated in relation to psychiatric disorders based on animal models and MRI techniques, the role of the anterior thalamus is less described.

Besides reciprocal connections with the cortex, the anterior nuclei of the thalamus also has direct inputs from the mammillary bodies and the hippocampal formation into different parts of the cingulate cortex, and form part of the Delay-Brion circuit (Metzger et al., 2013). Aggleton et al. (1999, 2010) proposed a hippocampal-anterior thalamic circuit mediating recall or recollection, and Van Der Werf et al. (2003) further confirmed the role of anterior thalamus in memory processing: amnesia following anteriorly located thalamic lesions

resembles the symptoms seen in hippocampal lesions. Therefore, altered development of hippocampal-anterior thalamic circuit may be a putative basis for the anteriorly located thalamic atrophy shown in our study, and provides an explanation to the impaired memory and learning performance of ex-preterm subjects, as seen in their later life (Isaacs et al., 2000; Peterson et al., 2000; Inder et al., 2005). Our study provides new anatomical support to the hypothesis that there are additional open circuit elements, other than the four previously mentioned closed loop frontal-subcortical circuits, that are at risk in preterm birth. Again, further validation is warranted in the future, ideally including the hippocampus and cingulate cortex in the correlation analysis.

4.2.3 Hemispheric asymmetrical vulnerability to preterm birth—Hemispheric asymmetry are well documented, with several higher cognitive functions, including language and auditory, lateralized in the cerebral cortex (Hutsler and Galuske, 2003). By analyzing mood disorders, several computed tomography based studies revealed a higher frequency and severity of depression in patients with left hemisphere lesions, most notably within the dorsolateral prefrontal-subcortical circuit (Robinson et al., 1984; Starkstein et al., 1987, 1988; Cummings, 1993). In a segmentation based MRI study investigating putamen and thalamus in patients with Alzheimer's disease (De Jong et al., 2008), left putaminal and thalamic volume changes were found to have a higher association with cognitive decline. As detected by our surface based morphometry analysis, significant prematurity associated changes are more prominent on the left thalamus, while fewer clusters with group differences are found on the right thalamus. Complementary to these results, the pose information we found in our study further confirms that the left thalamus and putamen may be more vulnerable to prematurity, in terms of significant or very low p-values in more than one pose parameters. Our study supports the concept that there are regional thalamic asymmetries in the preterm that may be related to subtle white matter injury, have prognostic significance, or be related to preterm birth itself.

4.3 Neuro-developmental considerations

The process of brain development is a complex sequence, and highly depends on timing. Apart from the general agreement that the earlier the preterm birth took place, the more severe the potential impact it will have on neurodevelopmental outcomes, more dedicated studies revealed a selective pattern of injury on brain structures with varied developmental time windows. Thalamic abnormalities in preterm birth are often attributed to the effect of ischemia and hypoxia, sepsis, or undernutrition on thalamo-cortical system development (Ball et al., 2012; Counsell et al., 2003, 2006). Recently, special attention has also been paid to the linked disturbance of subplate zone. The subplate zone serves as a 'waiting compartment' directing the in-growth of thalamocortical and basal forebrain fibers to the cortical plate, and injury or disturbances in this transient zone may result in far-reaching developmental effects (Volpe, 2009). The subplate zone starts its formation as early as 13–15 weeks of gestation, and undergoes a major enlargement in the second trimester (Mrzljak et al., 1988). After 26/27 weeks of gestation, the subplate zone gradually dissolves, but remains visible in the prefrontal cortex in newborns (Kostović et al., 2011). The existence of the subplate zone in the frontal cortex can last until sixth postnatal months, and some researchers believe that individual subplate-like neurons may be present until

adulthood (Kostovic et al., 1989). The wide developmental time window of the prefrontal cortex provides a neurodevelopmental substrate for its high vulnerability to preterm birth, and this is further confirmed by the prominent involvement of frontal cortex detected in our study.

The ingrowing of thalamocortical fibers from the medial dorsal nucleus (MD) of the thalamus into subplate zone starts as early as its formation period (Mrzljak et al., 1988), and the MD neurons were found to gradually reduced in differentiation after 28 gestational weeks by a transient cholinesterase (ChE) Staining study (Kostovic and Goldman-Rakic, 1983). That is to say, MD is a putative location affected by preterm birth, and the influence might present in a greater extent in very preterm birth (VPB) subjects, those born before 28 weeks of gestation, as the MD neurons still undergo massive differentiation. This is of particular relevance to our study, because MD area of the thalamus in our preterm subjects (average gestational age is 32.8 weeks) is smaller on average, but failed to reach a significant preterm vs. term difference, as elsewhere presented in studies investigating subjects with VPB or different level of brain injuries (Nagasunder et al., 2011).

In addition, although the group significant clusters limited within the anterior and ventral side of the thalamus, a widespread shrinkage in the preterm group is revealed in the average determinant and radius maps. As shown In Fig. 4, reduced volume of preterm group was presented in the majority of the thalamus nuclei, except for the left and right ventro-posterior nuclei. Ventro-posterior nuclei is involved in sensory input, which is considered to establish earlier in the brain development and therefore less vulnerable to preterm birth.

Furthermore, by comparing the significant clusters in correlation analysis with that in group difference analysis, we can see a different pattern of behaviors on the thalamus and the putamen. For the putamen, significant group difference clusters are mostly overlaid with the area that are significantly associated with thalamus atrophy, supporting the thoughts that the disturbances on the putamen are more a secondary effect of thalamic injury than a primary putaminal one. Whereas for the thalamus, significant group difference clusters do not fit well with the putaminal associated areas, and the only overlap confined to VA of the left thalamus. Other nuclei, like the anterior part of the thalamus, are not significantly correlated with putaminal volume, but also prone to atrophy in preterm infants. This reveals a more complicated pattern of thalamic disturbance: the altered development of the thalamus in premature infants cannot be completely attributed to the disturbance of the closed frontal-subcortical loop, as other open elements to the frontal-subcortical circuits, for example the hippocampus, may also reciprocally connected with the thalamus and subject to preterm associated atrophy. These findings support the thought of Volpe (2009), that thalamus undertakes dual type of injury during preterm birth, one from the preterm delivery associated disruption on thalamo-cortical pathways, and one from cortico-basal ganglia circuits passing through the pallidum of the ventral striatum. As a result, to our knowledge, our current study for the first time provides structural covariate evidence to depict the associated, albeit not identical patterns of vulnerability of thalamus and putamen in relation to prematurity.

4.4 Contribution and limitation of the study

The contributions of this study are threefold. First, we extend the localization power of subcortical structural analysis, and open the possibility to depict the effect of prematurity on the level of subnuclei of deep gray matter. Second, for the first time, we introduce the relative pose analysis into prematurity studies, and suggest that relative pose in subcortical structures is a useful indicator of brain injury, particularly in the process of development. Third, we investigate the associations between deep gray matter structures using the previously obtained surface and pose information, thus opening a new perspective of the investigation of specific and combined response of subcortical structures to brain disorders. The results presented in this paper may have implications for early prediction and long-term prognosis, which can be helped with implementing early specific behavior intervention for these preterm neonates, with the hope of reducing long term neurodevelopmental disabilities.

There are several limitations in our study: First, we need to use age at scan time as a covariate in our group analysis, due to a slight mismatch of age in the preterm and term groups. The use of linear regression does not rule out the possibility of a non-linear pattern of growth against gestational age. Second, birth weight has been demonstrated to be correlated with increased cognitive impairment (Foulder-Hughes and Cooke, 2003), and it may therefore affect the degree of alterations caused by preterm delivery. We did not include this information in the analysis, and we recognize this as a caveat of our study. Third, the inter-structural association analysis is limited to the most commonly affected deep gray matter areas. However, the cortex is intimately connected with the putamen and thalamus through cortical-basal ganglia and thalamo-cortical pathways, and the involvement of cerebral cortex in prematurity is well accepted. Therefore, the investigation of association of allied deep gray matter would be more comprehensive with the participant of the cerebral cortex. This will be the subject of our future work.

In the future, we will also like to apply this data set to a larger group of preterm neonates which have different types of clinical risk factors to see how these risk factors affect subcortical structure development. For example, it will be interesting to study the effect of chronic lung disease and necrotizing enterocolitis on subcortical structure development in preterms. It will be also useful to apply this methodology on preterm neonates with different degrees of perinatal white matter injury, which can give insight into the relationship between gray and white matter injuries. In addition, we will also apply the method to a longitudinal study of the same patients, thus allowing us to correlate the baseline results with long-term cognitive outcome, which will potentially yield important predictors of learning deficits in premature children.

Acknowledgments

We thank for the participation of families from Children's Hospital Los Angeles and Children's Hospital of Pittsburgh UPMC. This work was supported by the National Institutes of Health through NIH grant 5K23-NS063371 and grant R21EB012177 and R21AG043760.

References

- Abernethy LJ, Cooke RW, Foulder-Hughes L. Caudate and hippocampal volumes, intelligence, and motor impairment in 7-year-old children who were born preterm. *Pediatric research*. 2004; 55:884–893. [PubMed: 14764914]
- Aggleton JP, Brown MW. Episodic memory, amnesia, and the hippocampal-anterior thalamic axis. *Behavioral and Brain Sciences*. 1999; 22:425–444. [PubMed: 11301518]
- Aggleton JP, O’Mara SM, Vann SD, Wright NF, Tsanov M, Erichsen JT. Hippocampal–anterior thalamic pathways for memory: uncovering a network of direct and indirect actions. *European Journal of Neuroscience*. 2010; 31:2292–2307. [PubMed: 20550571]
- Alexander GE, Crutcher MD, DeLong MR. Basal ganglia-thalamocortical circuits: parallel substrates for motor, oculomotor, “prefrontal” and “limbic” functions. *Progress in brain research*. 1991; 85:119–146. [PubMed: 2094891]
- Allin M, Henderson M, Suckling J, Nosarti C, Rushe T, Fearon P, Stewart AL, Bullmore E, Rifkin L, Murray R. Effects of very low birthweight on brain structure in adulthood. *Developmental Medicine & Child Neurology*. 2004; 46:46–53. [PubMed: 14974647]
- Arsigny, V.; Commowick, O.; Pennec, X.; Ayache, N. *Medical Image Computing and Computer-Assisted Intervention–MICCAI 2006*. Springer; 2006. A log-euclidean framework for statistics on diffeomorphisms; p. 924-931.
- Ball G, Boardman JP, Rueckert D, Aljabar P, Arichi T, Merchant N, Gousias IS, Edwards AD, Counsell SJ. The effect of preterm birth on thalamic and cortical development. *Cerebral Cortex*. 2012; 22:1016–1024. [PubMed: 21772018]
- Bechara A, Tranel D, Damasio H. Characterization of the decision-making deficit of patients with ventromedial prefrontal cortex lesions. *Brain*. 2000; 123:2189–2202. [PubMed: 11050020]
- Bhutta AT, Cleves MA, Casey PH, Cradock MM, Anand K. Cognitive and behavioral outcomes of school-aged children who were born preterm. *JAMA: the journal of the American Medical Association*. 2002; 288:728–737. [PubMed: 12169077]
- Boardman JP, Counsell SJ, Rueckert D, Kapellou O, Bhatia KK, Aljabar P, Hajnal J, Allsop JM, Rutherford MA, Edwards AD. Abnormal deep grey matter development following preterm birth detected using deformation-based morphometry. *Neuroimage*. 2006; 32:70–78. [PubMed: 16675269]
- Boardman JP, Craven C, Valappil S, Counsell SJ, Dyet L, Rueckert D, Aljabar P, Rutherford MA, Chew A, Allsop JM, et al. A common neonatal image phenotype predicts adverse neurodevelopmental outcome in children born preterm. *Neuroimage*. 2010; 52:409–414. [PubMed: 20451627]
- Bossa M, Zacur E, Olmos S. Statistical analysis of relative pose information of subcortical nuclei: application on adni data. *Neuroimage*. 2011; 55:999–1008. [PubMed: 21216295]
- Bossa MN, Olmos S. Statistical model of similarity transformations: Building a multi-object pose model of brain structures. *IEEE Comput Soc Workshop Math Methods Biomed Image Anal*. 2006:59.
- Buchmayer S, Johansson S, Johansson A, Hultman CM, Sparén P, Cnattingius S. Can association between preterm birth and autism be explained by maternal or neonatal morbidity? *Pediatrics*. 2009; 124:e817–e825. [PubMed: 19841112]
- Caravale B, Tozzi C, Albino G, Vicari S. Cognitive development in low risk preterm infants at 3–4 years of life. *Archives of Disease in Childhood-Fetal and Neonatal Edition*. 2005; 90:F474–F479. [PubMed: 15956096]
- Casanova MF, El-Baz AS, Kamat SS, Dombroski BA, Khalifa F, Elnakib A, Soliman A, Allison-McNutt A, Switala AE. Focal cortical dysplasias in autism spectrum disorders. *Acta neuropathologica communications*. 2013; 1:67. [PubMed: 24252498]
- Cheon KA, Kim YS, Oh SH, Park SY, Yoon HW, Herrington J, Nair A, Koh YJ, Jang DP, Kim YB, et al. Involvement of the anterior thalamic radiation in boys with high functioning autism spectrum disorders: a diffusion tensor imaging study. *Brain research*. 2011; 1417:77–86. [PubMed: 21890117]

- Counsell SJ, Allsop JM, Harrison MC, Larkman DJ, Kennea NL, Kapellou O, Cowan FM, Hajnal JV, Edwards AD, Rutherford MA. Diffusion-weighted imaging of the brain in preterm infants with focal and diffuse white matter abnormality. *Pediatrics*. 2003; 112:1–7. [PubMed: 12837859]
- Counsell SJ, Shen Y, Boardman JP, Larkman DJ, Kapellou O, Ward P, Allsop JM, Cowan FM, Hajnal JV, Edwards AD, et al. Axial and radial diffusivity in preterm infants who have diffuse white matter changes on magnetic resonance imaging at term-equivalent age. *Pediatrics*. 2006; 117:376–386. [PubMed: 16452356]
- Cummings JL. Frontal-subcortical circuits and human behavior. *Archives of neurology*. 1993; 50:873. [PubMed: 8352676]
- De Jong L, Van Der Hiele K, Veer I, Houwing J, Westendorp R, Bollen E, De Bruin P, Middelkoop H, Van Buchem M, Van Der Grond J. Strongly reduced volumes of putamen and thalamus in alzheimer's disease: an mri study. *Brain*. 2008; 131:3277–3285. [PubMed: 19022861]
- Draganski B, Kherif F, Klöppel S, Cook PA, Alexander DC, Parker GJ, Deichmann R, Ashburner J, Frackowiak RS. Evidence for segregated and integrative connectivity patterns in the human basal ganglia. *The Journal of Neuroscience*. 2008; 28:7143–7152. [PubMed: 18614684]
- Dryden, I.; Mardia, K. *Statistical analysis of shape*. Wiley; 1998.
- Fily A, Pierrat V, Delporte V, Breart G, Truffert P, et al. Factors associated with neurodevelopmental outcome at 2 years after very preterm birth: the population-based nord-pas-de-calais epipage cohort. *Pediatrics*. 2006; 117:357–366. [PubMed: 16452354]
- Flamand VH, Nadeau L, Schneider C. Brain motor excitability and visuomotor coordination in 8-year-old children born very preterm. *Clinical Neurophysiology*. 2012; 123:1191–1199. [PubMed: 22018705]
- Foulder-Hughes LA, Cooke R. Motor, cognitive, and behavioural disorders in children born very preterm. *Developmental Medicine & Child Neurology*. 2003; 45:97–103. [PubMed: 12578235]
- Golden JA, Harding BN. Cortical malformations: unfolding polymicrogyria. *Nature Reviews Neurology*. 2010; 6:471–472.
- Goldman-Rakic PS. Circuitry of primate prefrontal cortex and regulation of behavior by representational memory. *Comprehensive Physiology*. 1987
- Gorcowski K, Styner M, Jeong JY, Marron J, Piven J, Hazlett HC, Pizer SM, Gerig G. Multi-object analysis of volume, pose, and shape using statistical discrimination. *Pattern Analysis and Machine Intelligence, IEEE Transactions on*. 2010; 32:652–661.
- Groenewegen HJ, Berendse HW. The specificity of the 'nonspecific' midline and intralaminar thalamic nuclei. *Trends in neurosciences*. 1994; 17:52–57. [PubMed: 7512768]
- Grunau RE, Whitfield MF, Davis C. Pattern of learning disabilities in children with extremely low birth weight and broadly average intelligence. *Archives of pediatrics & adolescent medicine*. 2002; 156:615. [PubMed: 12038896]
- Haber SN. The primate basal ganglia: parallel and integrative networks. *Journal of chemical neuroanatomy*. 2003; 26:317–330. [PubMed: 14729134]
- Hart AR, Whitby EW, Griffiths PD, Smith MF. Magnetic resonance imaging and developmental outcome following preterm birth: review of current evidence. *Developmental Medicine & Child Neurology*. 2008; 50:655–663. [PubMed: 18754914]
- Hattie, J. *Visible learning: A synthesis of over 800 meta-analyses relating to achievement*. Routledge; 2008.
- Hotelling H. The generalization of student's ratio. *The Annals of Mathematical Statistics*. 1931; 2:360–378.
- Hutsler J, Galuske RA. Hemispheric asymmetries in cerebral cortical networks. *Trends in neurosciences*. 2003; 26:429–435. [PubMed: 12900174]
- Inder TE, Warfield SK, Wang H, Hüppi PS, Volpe JJ. Abnormal cerebral structure is present at term in premature infants. *Pediatrics*. 2005; 115:286–294. [PubMed: 15687434]
- Isaacs EB, Lucas A, Chong WK, Wood SJ, Johnson CL, Marshall C, Vargha-Khadem F, Gadian DG. Hippocampal volume and everyday memory in children of very low birth weight. *Pediatric research*. 2000; 47:713–720. [PubMed: 10832727]

- Joseph RM, Tager-Flusberg H. The relationship of theory of mind and executive functions to symptom type and severity in children with autism. *Development and psychopathology*. 2004; 16:137–155. [PubMed: 15115068]
- Karcher H. Riemannian center of mass and mollifier smoothing. *Communications on pure and applied mathematics*. 1977; 30:509–541.
- Kesler SR, Ment LR, Vohr B, Pajot SK, Schneider KC, Katz KH, Ebbitt TB, Duncan CC, Makuch RW, Reiss AL. Volumetric analysis of regional cerebral development in preterm children. *Pediatric neurology*. 2004; 31:318–325. [PubMed: 15519112]
- Kesler SR, Reiss AL, Vohr B, Watson C, Schneider KC, Katz KH, Maller-Kesselman J, Silbereis J, Constable RT, Makuch RW, et al. Brain volume reductions within multiple cognitive systems in male preterm children at age twelve. *The Journal of pediatrics*. 2008; 152:513–520. [PubMed: 18346506]
- Klein JC, Rushworth MF, Behrens TE, Mackay CE, de Crespigny AJ, D'Arceuil H, Johansen-Berg H. Topography of connections between human prefrontal cortex and mediodorsal thalamus studied with diffusion tractography. *Neuroimage*. 2010; 51:555–564. [PubMed: 20206702]
- Kostovic I, Goldman-Rakic PS. Transient cholinesterase staining in the mediodorsal nucleus of the thalamus and its connections in the developing human and monkey brain. *Journal of Comparative Neurology*. 1983; 219:431–447. [PubMed: 6196382]
- Kostovi I, Judaš M, Sedmak G. Developmental history of the subplate zone, subplate neurons and interstitial white matter neurons: relevance for schizophrenia. *International Journal of Developmental Neuroscience*. 2011; 29:193–205. [PubMed: 20883772]
- Kostovi I, Lukinovi N, Judaš M, Bogdanovi N, Mrzljak L, Zečević N, Kubat M. Structural basis of the developmental plasticity in the human cerebral cortex: the role of the transient subplate zone. *Metabolic brain disease*. 1989; 4:17–23. [PubMed: 2649779]
- Lao Y, Shi J, Wang Y, Ceschin R, Hwang D, Nelson M, Panigrahy A, Lepore N. Statistical analysis of relative pose of the thalamus in preterm neonates. *MICCAI workshop on Clinical Image-based Procedures*. 2013
- Lepore N, Brun C, Chou YY, Chiang MC, Dutton RA, Hayashi KM, Luders E, Lopez OL, Aizenstein HJ, Toga AW, et al. Generalized tensor-based morphometry of hiv/aids using multivariate statistics on deformation tensors. *Medical Imaging, IEEE Transactions on*. 2008; 27:129–141.
- Limperopoulos C, Bassan H, Sullivan NR, Soul JS, Robertson RL, Moore M, Ringer SA, Volpe JJ, du Plessis AJ. Positive screening for autism in ex-preterm infants: prevalence and risk factors. *Pediatrics*. 2008; 121:758–765. [PubMed: 18381541]
- Lin Y, Okumura A, Hayakawa F, Kato T, Kuno K, Watanabe K. Quantitative evaluation of thalamic and basal ganglia in infants with periventricular leukomalacia. *Developmental Medicine & Child Neurology*. 2001; 43:481–485. [PubMed: 11463180]
- Marlow N, Wolke D, Bracewell MA, Samara M. Neurologic and developmental disability at six years of age after extremely preterm birth. *New England Journal of Medicine*. 2005; 352:9–19. [PubMed: 15635108]
- Mega MS, Cummings JL. Frontal-subcortical circuits and neuropsychiatric disorders. *Neurosciences*. 1994; 6:358–370.
- Metzger CD, van der Werf YD, Walter M. Functional mapping of thalamic nuclei and their integration into cortico-striatal-thalamo-cortical loops via ultra-high resolution imaging—from animal anatomy to in vivo imaging in humans. *Frontiers in neuroscience*. 2013; 7
- Mrzljak L, Uylings H, Kostovic I, van Eden CG. Prenatal development of neurons in the human prefrontal cortex: I. a qualitative golgi study. *Journal of comparative neurology*. 1988; 271:355–386. [PubMed: 2454966]
- Nagasunder A, Kinney H, Blüml S, Tavaré C, Rosser T, Gilles F, Nelson M, Panigrahy A. Abnormal microstructure of the atrophic thalamus in preterm survivors with periventricular leukomalacia. *American Journal of Neuroradiology*. 2011; 32:185–191. [PubMed: 20930003]
- Nichols TE, Holmes AP. Nonparametric permutation tests for functional neuroimaging: a primer with examples. *Human brain mapping*. 2001; 15:1–25. [PubMed: 11747097]
- Pennec X, Fillard P, Ayache N. A riemannian framework for tensor computing. *International Journal of Computer Vision*. 2006; 66:41–66.

- Peterson BS, Vohr B, Staib LH, Cannistraci CJ, Dolberg A, Schneider KC, Katz KH, Westerveld M, Sparrow S, Anderson AW, et al. Regional brain volume abnormalities and long-term cognitive outcome in preterm infants. *JAMA: the journal of the American Medical Association*. 2000; 284:1939–1947. [PubMed: 11035890]
- Pizer SM, Fritsch DS, Yushkevich PA, Johnson VE, Chaney EL. Segmentation, registration, and measurement of shape variation via image object shape. *Medical Imaging, IEEE Transactions on*. 1999; 18:851–865.
- Reijneveld SA, De Kleine M, van Baar AL, Kollée LA, Verhaak CM, Verhulst FC, Verloove-Vanhorick SP. Behavioural and emotional problems in very preterm and very low birthweight infants at age 5 years. *Archives of Disease in Childhood-Fetal and Neonatal Edition*. 2006; 91:F423–F428. [PubMed: 16877476]
- Robinson RG, Kubos KL, Starr LB, Rao K, Price TR. Mood disorders in stroke patients: importance of location of lesion. *Brain*. 1984; 107:81–93. [PubMed: 6697163]
- Robinson S, Goddard L, Dritschel B, Wisley M, Howlin P. Executive functions in children with autism spectrum disorders. *Brain and Cognition*. 2009; 71:362–368. [PubMed: 19628325]
- Ross, A. Procrustes analysis Course report. Department of Computer Science and Engineering, University of South Carolina; 2004.
- Shi J, Wang Y, Ceschin R, An X, Lao Y, Vanderbilt D, Nelson MD, Thompson PM, Panigrahy A, Leporé N. A multivariate surface-based analysis of the putamen in premature newborns: Regional differences within the ventral striatum. *PloS one*. 2013; 8:e66736. [PubMed: 23843961]
- Shi J, Wang Y, Ceschin R, An X, Nelson MD, Panigrahy A, Leporé N. Surface fluid registration and multivariate tensor-based morphometry in newborns—the effects of prematurity on the putamen. *APSIPA Annual Summit and Conference*. 2012
- Sonuga-Barke EJ. Psychological heterogeneity in ad/hd—a dual pathway model of behaviour and cognition. *Behavioural brain research*. 2002; 130:29–36. [PubMed: 11864715]
- Srinivasan L, Dutta R, Counsell SJ, Allsop JM, Boardman JP, Rutherford MA, Edwards AD. Quantification of deep gray matter in preterm infants at term-equivalent age using manual volumetry of 3-tesla magnetic resonance images. *Pediatrics*. 2007; 119:759–765. [PubMed: 17403847]
- Starkstein SE, Robinson RG, Berthier ML, Parikh RM, Price TR. Differential mood changes following basal ganglia vs thalamic lesions. *Archives of Neurology*. 1988; 45:725. [PubMed: 3390026]
- Starkstein SE, Robinson RG, Price TR. Comparison of cortical and subcortical lesions in the production of poststroke mood disorders. *Brain*. 1987; 110:1045–1059. [PubMed: 3651794]
- Strand-Brodd K, Ewald U, Grönqvist H, Holmström G, Strömberg B, Grönqvist E, von Hofsten C, Rosander K. Development of smooth pursuit eye movements in very preterm infants: 1. general aspects. *Acta Paediatrica*. 2011; 100:983–991. [PubMed: 21332783]
- Thompson PM, Hayashi KM, de Zubicaray GI, Janke AL, Rose SE, Semple J, Hong MS, Herman DH, Gravano D, Doddrell DM, et al. Mapping hippocampal and ventricular change in alzheimer disease. *Neuroimage*. 2004; 22:1754–1766. [PubMed: 15275931]
- Toplak ME, Jain U, Tannock R. Executive and motivational processes in adolescents with attention-deficit-hyperactivity disorder (adhd). *Behavioral and Brain Functions*. 2005; 1:8. [PubMed: 15982413]
- Van Der Werf YD, Jolles J, Witter MP, Uylings H. Contributions of thalamic nuclei to declarative memory functioning. *Cortex*. 2003; 39:1047–1062. [PubMed: 14584566]
- Volpe JJ. Brain injury in premature infants: a complex amalgam of destructive and developmental disturbances. *The Lancet Neurology*. 2009; 8:110–124. [PubMed: 19081519]
- Wang, Y. Multivariate surface-based subcortical structure morphometry system. 2011d. <http://gsl.lab.asu.edu/conformal.htm>
- Wang Y, Panigrahy A, Ceschin R, Liu S, Thompson PM, Lepore N. Surface morphometry of subcortical structures in premature neonates. *Proc Intl Soc Mag Reson Med*. 2011a:2585.
- Wang, Y.; Panigrahy, A.; Shi, J.; Ceschin, R.; Nelson, M. Multivariate tensor based morphometry on premature neonates: a pilot study. *Proceedings of the MICCAI workshop on Image Analysis of Human Brain Development (IAHBD 2011)*; 2011b.

- Wang Y, Song Y, Rajagopalan P, An T, Liu K, Chou YY, Gutman B, Toga AW, Thompson PM. Surface-based tbm boosts power to detect disease effects on the brain: An n = 804 adni study. *Neuroimage*. 2011c; 56:1993–2010. [PubMed: 21440071]
- Wang Y, Zhang J, Gutman B, Chan TF, Becker JT, Aizenstein HJ, Lopez OL, Tamburo RJ, Toga AW, Thompson PM. Multivariate tensor-based morphometry on surfaces: Application to mapping ventricular abnormalities in hiv/aids. *NeuroImage*. 2010a; 49:2141–2157. [PubMed: 19900560]
- Wood NS, Marlow N, Costeloe K, Gibson AT, Wilkinson AR. Neurologic and developmental disability after extremely preterm birth. *New England Journal of Medicine*. 2000; 343:378–384. [PubMed: 10933736]
- Zhang H, Yushkevich PA, Alexander DC, Gee JC, et al. Deformable registration of diffusion tensor mr images with explicit orientation optimization. *Medical image analysis*. 2006; 10:764–785. [PubMed: 16899392]

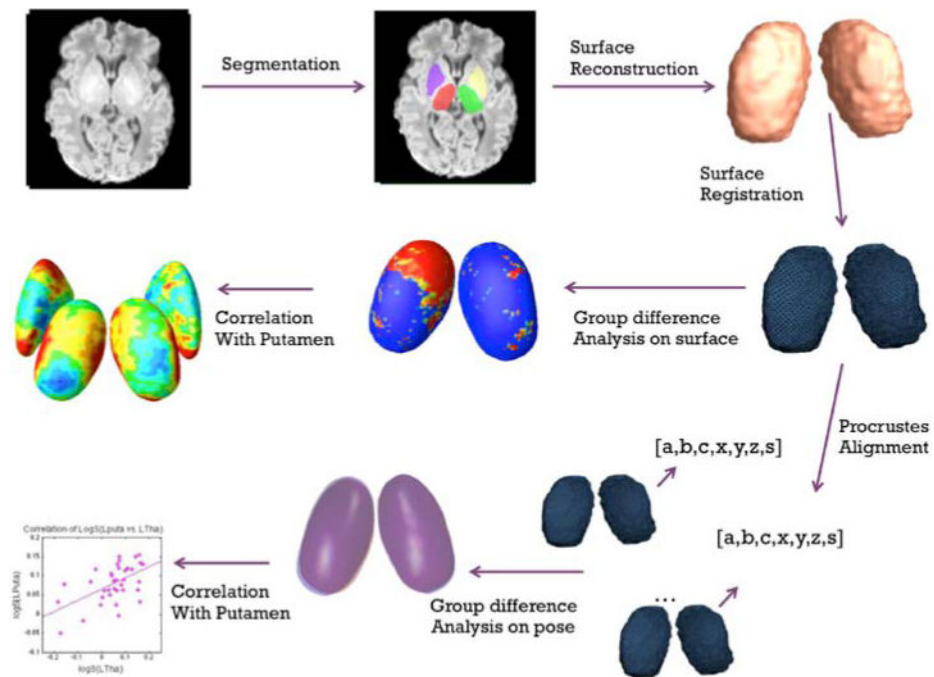


Fig. 1. Diagram of the combined shape and relative pose analysis. For simplicity, only the surfaces of thalamus are used for illustration. Top Row: the subcortical structures are first segmented from T1 images, and then reconstructed to 3D surface models; Middle Row: surface based morphometry and correlation analysis; Bottom Row: relative pose based statistics and correlation analysis

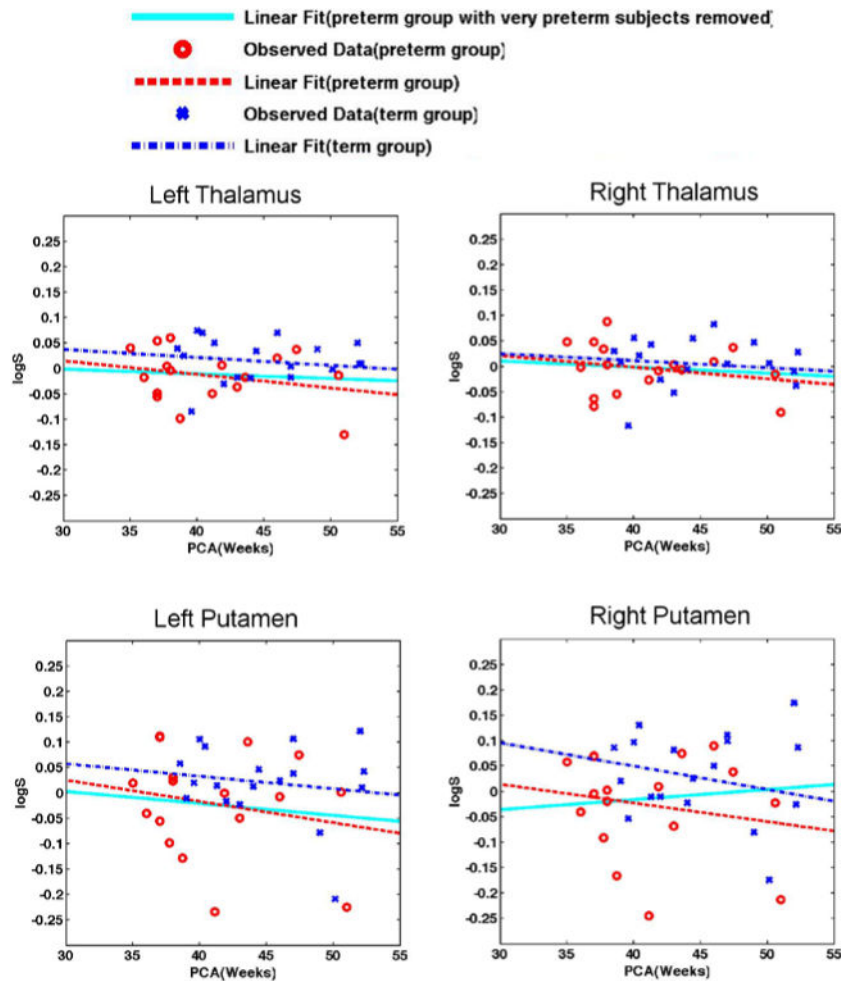


Fig. 2. Distribution of scale parameter in log-Euclidean space ($\log S$) for the left thalamus, right thalamus, left putamen, and right putamen. Scatter points in the figure represent observed results from the Procrustes alignment, while lines represent their corresponding linear regressions. In all the figures above, data from the preterm group are marked in red (circles and dash lines), and while that from the term group are marked in blue (x symbols and dash-dot lines). Note that the $\log S$ for the preterm group are distributed lower in the graphs, compared to that from the term controls, indicating a smaller size of structures in the preterm group. When very preterm subjects are removed from the sample (gestational age at birth < 31 weeks), the downward trends of linear regression (shown in solid cyan lines) for preterm subjects disappears, indicating a closer size compared to the term born subjects.

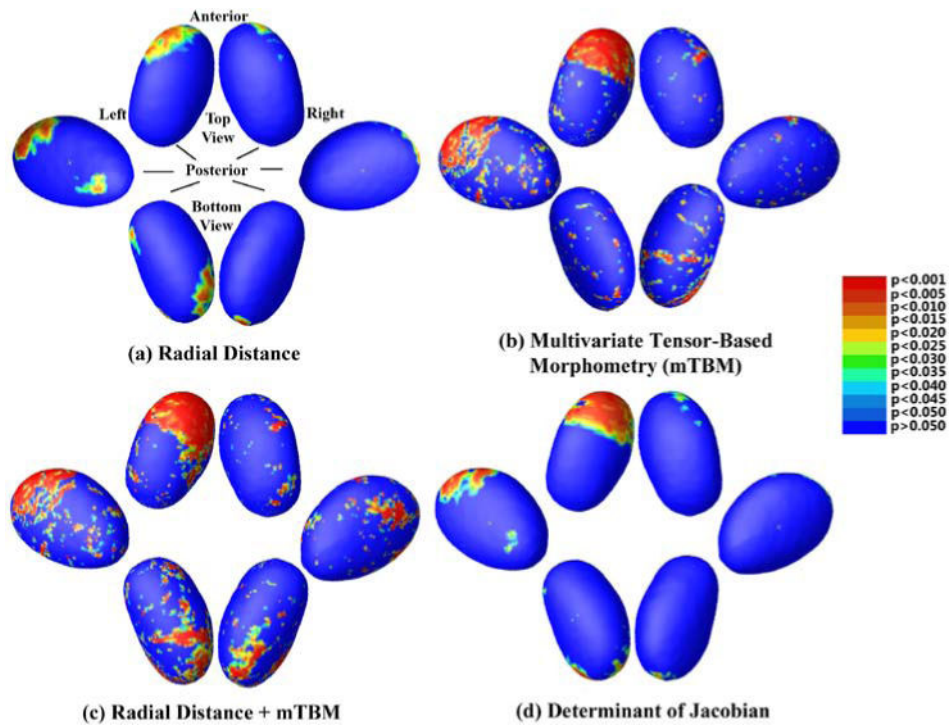


Fig. 3. Thalamus statistical p -maps: Overall p -values are $p=0.0901$ for MAD(a), $p=0.0077$ for mTBM(b), $p=0.0035$ for MAD + mTBM(c) and $p=0.0683$ for $\det J$ (d)

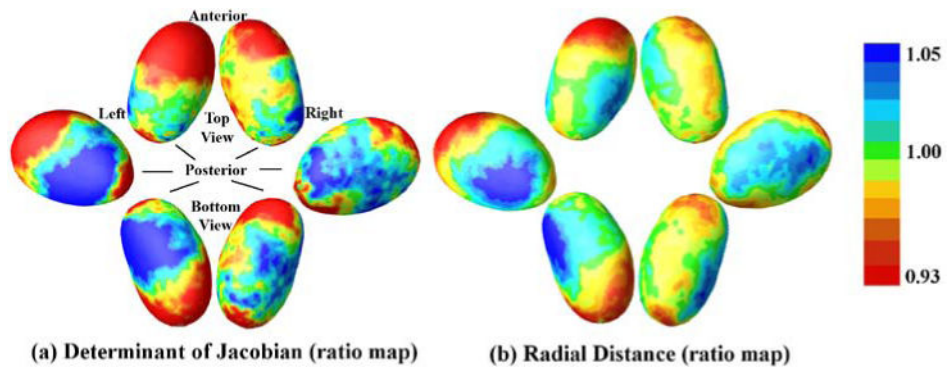


Fig. 4. Vertex-wise ratio determinant (a) and radial distance (b) maps of the thalamus. Widespread shrinkage of preterm group is present in both thalami, and the clusters with significant preterm vs. term differences (seen in Fig. 3) all fall on the preterm < term areas

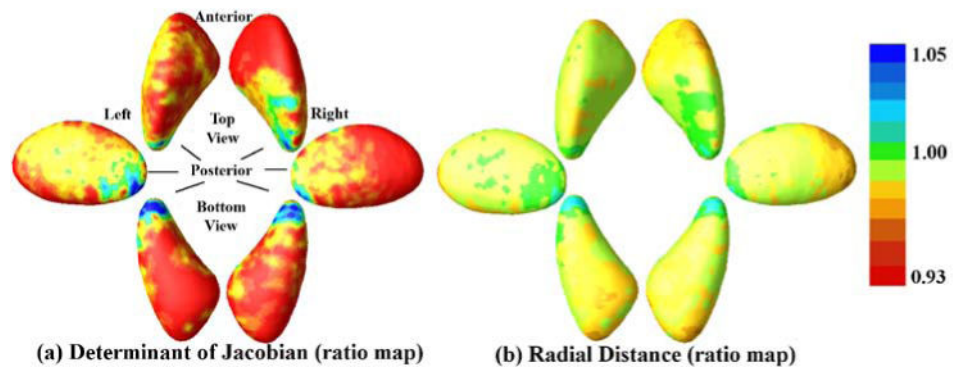


Fig. 5. Vertex-wise ratio determinant (a) and radial distance (b) maps of putamen. Widespread shrinkage of preterm group is present in both putamen, and the clusters with significant preterm vs. term differences (seen in our previous publication (Shi et al., 2013)) mostly fall on the preterm < term areas

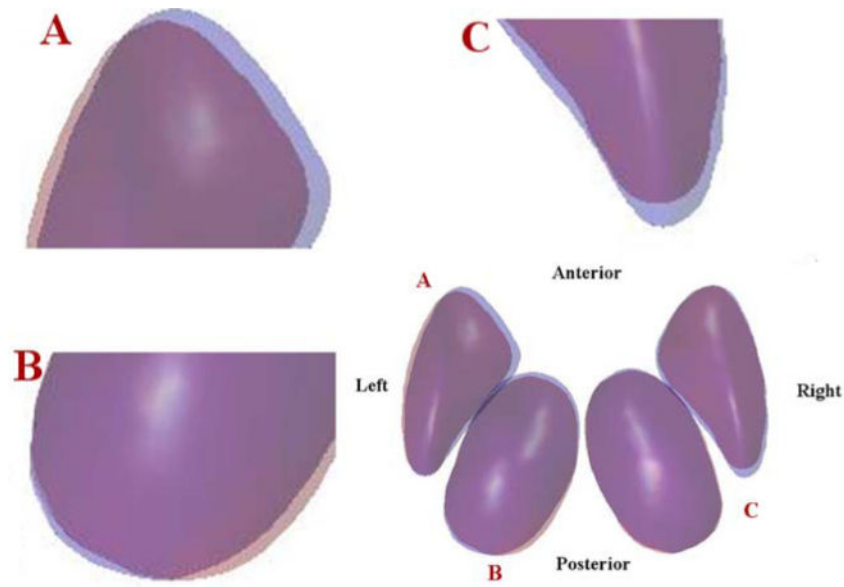


Fig. 6. 3D visualization of the pose of mean shapes averaged from the preterm (red) and term groups (blue). Areas where the mean shapes of two groups overlaid appear in purple. To better visualize the pose changes, enlargements of locations A, B, C at the bottom right figure are presented in top left, bottom left, and top right figures, respectively. Note the borders of these two structures: shift of pose are evident on the left putamen (A), left thalamus (B), and right putamen (C), but are quite small the right thalamus

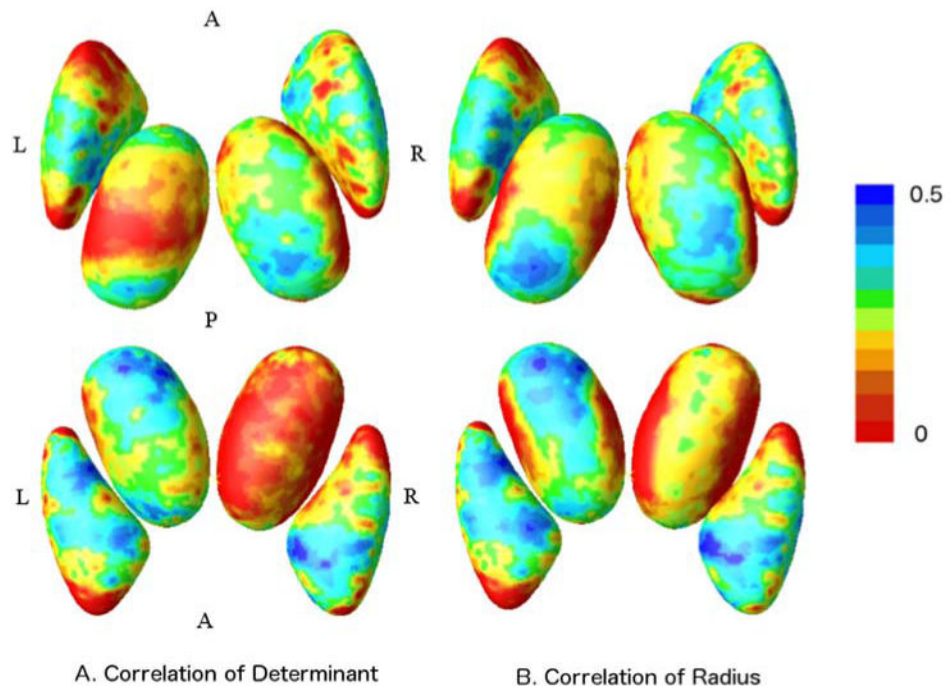
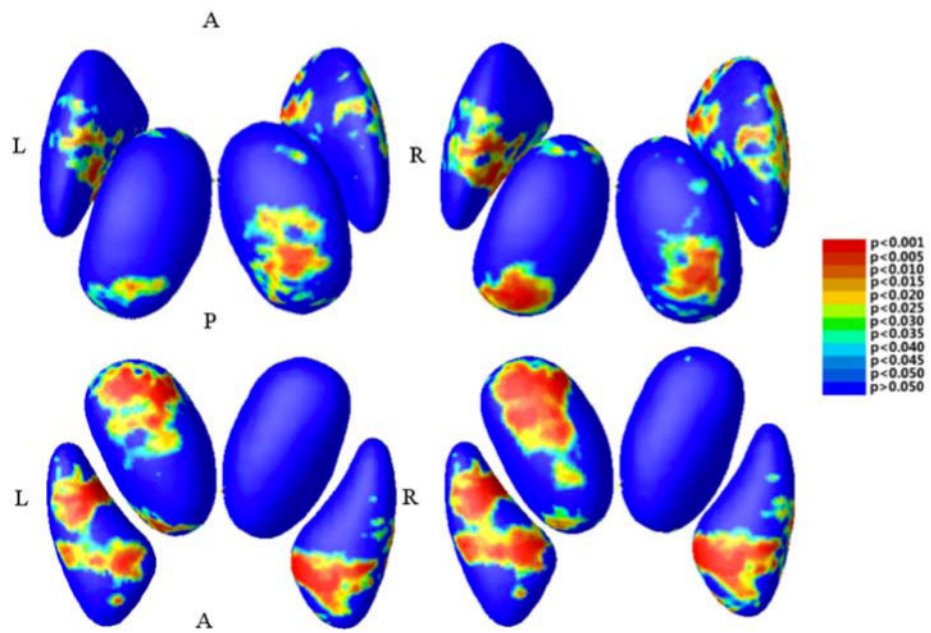


Fig. 7. Vertex-wise correlation coefficient maps have been generated based on determinant (left) and radius (right), respectively. The upper row are displayed in a superior view, while the bottom ones are seen from the inferior brain surface



A. P map for the Correlation of Determinant B. P map for the Correlation of Radius

Fig. 8. P-maps of the corresponding to the correlation coefficients, derived from the determinant map (left), and radius maps (right). The upper row are displayed in a superior view, while the bottom are seen from the inferior brain surface

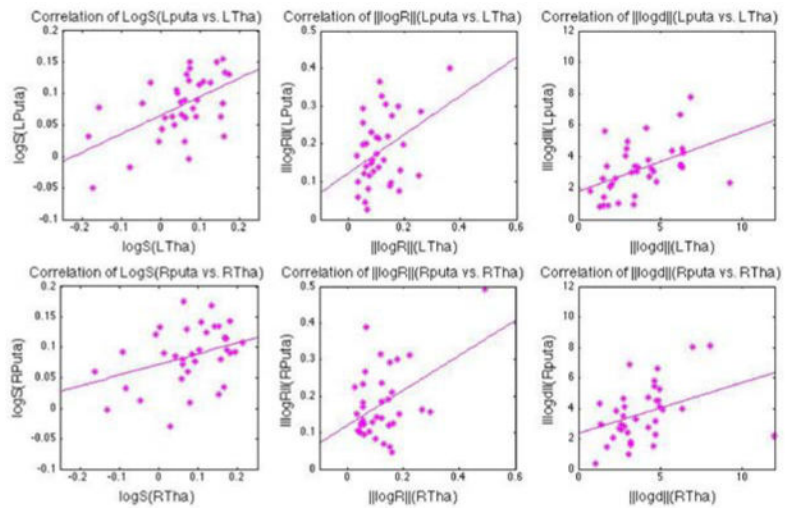


Fig. 9.

The correlation between the thalamus and the putamen in the left (upper row) and right (bottom row) hemispheres, tested using pose parameters: $\log S$ (left column), $\| \log R \|$ (middle column), $\| \log d \|$ (right column). More details, such as correlation coefficients and p -values, are presented in Table 2

Table 1

p-values of statistical analyses on pose parameters. 6 sets of parameters characterizing relative pose of left thalamus (LTha), right thalamus (RTha), left putamen (LPut), and right putamen (RPut) are investigated here using univariate and multivariate analyses. Parameters are categorized as *logS*, $\|logR\|$, $\|logd\|$ for univariate tests, and as $(\theta_x, \theta_y, \theta_z)$, (x, y, z) , and a combination of 7 parameters for multivariate tests. All the *p*-values are obtained after permutation testing. Significant *p*-values ($p < 0.05$) are highlighted in cyan, while *p*-values that are interestingly low but failed to reach significance are highlighted in yellow.

Pose Parameters	LTha	RTha	LPut	RPut
<i>logS</i>	2.36e-02	3.37e-01	7.50e-02	3.28e-02
$\ logR\ $	7.80e-01	5.22e-01	1.92e-01	9.75e-01
$\ logd\ $	9.01e-01	3.66e-01	9.67e-02	4.41e-01
$(\theta_x, \theta_y, \theta_z)$	1.06e-02	7.16e-01	6.71e-02	3.61e-01
(x, y, z)	8.26e-01	8.15e-01	8.71e-01	3.14e-01
All7parameters	2.16e-02	9.12e-01	1.90e-01	3.49e-01

Table 2

Correlation results based on pose parameters. 4 sets of correlation results based on pose parameters: $\log S$, $\|\log R\|$, $\|\log d\|$, between 2 thalami and 2 putamen. Both coefficients and p values are provided in each of the test, with significant correlations highlighted in babypink. Here, we set the significance with $p < 0.01$.

	$\log S$	$\ \log R\ $	$\ \log d\ $
LPut vs. LTha	$\beta=5.45, p=5.00e-04$	$\beta=3.94, p=1.55e-02$	$\beta=4.61, p=4.10e-03$
RPut vs. LTha	$\beta=6.13, p<1.00e-04$	$\beta=2.79, p=1.01e-01$	$\beta=3.58, p=3.50e-02$
LPut vs. RTha	$\beta=3.05, p=7.59e-02$	$\beta=4.19, p=1.25e-02$	$\beta=4.61, p=3.30e-03$
RPut vs. RTha	$\beta=3.61, p=3.12e-02$	$\beta=4.52, p=9.90e-03$	$\beta=3.74, p=2.59e-02$